Contrasting responses within a single neuron class enable sex-specific attraction in *Caenorhabditis elegans*

Anusha Narayan[a,b,c], Vivek Venkatachalam[d], Omer Durak[a,b,e], Douglas K. Reilly[f], Neelanjan Bose[g], Frank C. Schroeder[g], Aravinthan D. T. Samuel[d], Jagan Srinivasan[a,b,f,1], and Paul W. Sternberg[a,b,1]

[a]Howard Hughes Medical Institute, California Institute of Technology, Pasadena, CA 91125; [b]Division of Biology and Biological Engineering, California Institute of Technology, Pasadena, CA 91125; [c]Department of Brain and Cognitive Sciences, McGovern Institute for Brain Research, Massachusetts Institute of Technology, Cambridge, MA 02139; [d]Center for Brain Science and Department of Physics, Harvard University, Cambridge, MA 02138; [e]Neuroscience Graduate Program, Massachusetts Institute of Technology, Cambridge, MA 02139; [f]Department of Biology and Biotechnology, Worcester Polytechnic Institute, Worcester, MA 01609; and [g]Boyce Thompson Institute and Department of Chemistry and Chemical Biology, Cornell University, Ithaca, NY 14853

Contributed by Paul W. Sternberg, January 22, 2016 (sent for review July 5, 2015; reviewed by Mala Murthy and Douglas Portman)

Animals find mates and food, and avoid predators, by navigating to regions within a favorable range of available sensory cues. How are these ranges set and recognized? Here we show that male *Caenorhabditis elegans* exhibit strong concentration preferences for sex-specific small molecule cues secreted by hermaphrodites, and that these preferences emerge from the collective dynamics of a single male-specific class of neurons, the cephalic sensory neurons (CEMs). Within a single worm, CEM responses are dissimilar, not determined by anatomical classification and can be excitatory or inhibitory. Response kinetics vary by concentration, suggesting a mechanism for establishing preferences. CEM responses are enhanced in the absence of synaptic transmission, and worms with only one intact CEM show nonpreferential attraction to all concentrations of ascaroside for which CEM is the primary sensor, suggesting that synaptic modulation of CEM responses is necessary for establishing preferences. A heterogeneous concentration-dependent sensory representation thus appears to allow a single neural class to set behavioral preferences and recognize ranges of sensory cues.

population coding | electrophysiology | chemosensation | calcium imaging | animal behavior

The chemical senses of taste and smell are an important source of sensory input for organisms from worms to humans, and elements of the olfactory system are evolutionarily conserved across metazoa (1, 2). The neural mechanisms of olfactory processing are a subject of active research (3), and much is known about the encoding of odor identity and concentration (4–6). However, the issue of ranges of favorable odor concentrations has been less studied. A reasonable general hypothesis is that physical sensory limitations set perceptual boundaries, limiting the range of an animal to respond favorably. However, there are instances where differences in odor concentrations can have different meanings: For example, both male and female rodents produce the same pheromone at different concentrations (7), and so males need to be able to distinguish between low and high concentrations. Similarly, a very high concentration might signal an adverse environment with overcrowding, in which case the animal is better off looking elsewhere. In such cases, the concentration preferences of the animals are tuned to some optimal value that has a higher probability of a successful outcome. Here, we show that *Caenorhabditis elegans* exhibits a striking tuning of pheromone concentration preferences, and that this concentration tuning is actively built and maintained by a single class of male-specific neurons, the cephalic sensory neurons (CEMs).

The nervous system of *C. elegans* is famously compact, with 302 hermaphrodite neurons grouped into 118 classes based on morphology and connectivity (8), and 385 male neurons (9–11). Some classes of neurons are sex-specific (Fig. 1*A*). Members of a class are typically distinguished from each other by their relative anatomical position, such as left/right and dorsal/ventral. Although initially it was thought that members of a class were functionally similar, several studies have revealed asymmetry in the responses of members of a class, in particular the sensory neurons (12, 13).

The four male-specific CEM neurons are considered members of a single class based on substantial evidence: their fourfold symmetric location of cell bodies (14), the morphology of their processes (15), the morphology of their nuclei (16) and their cilia (17), and their gene expression (15, 18, 19). Presumptive CEMs die in the hermaphrodite (20) and are under coordinated genetic control, although the ventral CEMs are less sensitive to sex-specific apoptosis (16).

Chemical analyses of hermaphrodite secretions by mass spectroscopy and 2D NMR spectroscopy have discovered a novel family of small molecules called ascarosides (21–23), which serve diverse biological functions (24). Certain ascarosides secreted by hermaphrodites are attractive exclusively to males, which exhibit strong concentration preferences (23). We mapped the behavioral concentration tuning curve and ablated individual neurons to identify the mediators of this response. We next performed electrophysiological, calcium imaging, and genetic analyses to uncover the sensory coding strategy that allows *C. elegans* to

Significance

Roundworms carry out crucial sensory behaviors with a relatively small number of neurons. We find that male roundworms have strong preferences for particular concentrations of sex-specific small molecule cues secreted by their potential mates. These preferences emerge from the dynamics of a population of four apparently identical male-specific neurons. The response of these sensory neurons is not uniform, with some being excitatory and others inhibitory, and the timing of response varies with concentration. These features allow this single neuronal class to prefer a concentration, and potentially to calculate a derivative of chemical concentration. This previously uncharacterized neural coding strategy might allow nematodes to efficiently use a small number of cells to carry out a crucial computation to enact innate social behaviors.

Author contributions: A.N. and J.S. designed research; A.N., O.D., D.K.R., N.B., F.C.S., and J.S. performed research; A.N., V.V., A.D.T.S., J.S., and P.W.S. analyzed data; A.N., V.V., A.D.T.S., J.S., and P.W.S. wrote the paper; and N.B. and F.C.S. synthesized ascr#3 and #8.

Reviewers: M.M., Princeton University; and D.P., University of Rochester Medical Center.

The authors declare no conflict of interest.

[1]To whom correspondence may be addressed. Email: pws@caltech.edu or jsrinivasan@wpi.edu.

This article contains supporting information online at www.pnas.org/lookup/suppl/doi:10.1073/pnas.1600786113/-/DCSupplemental.

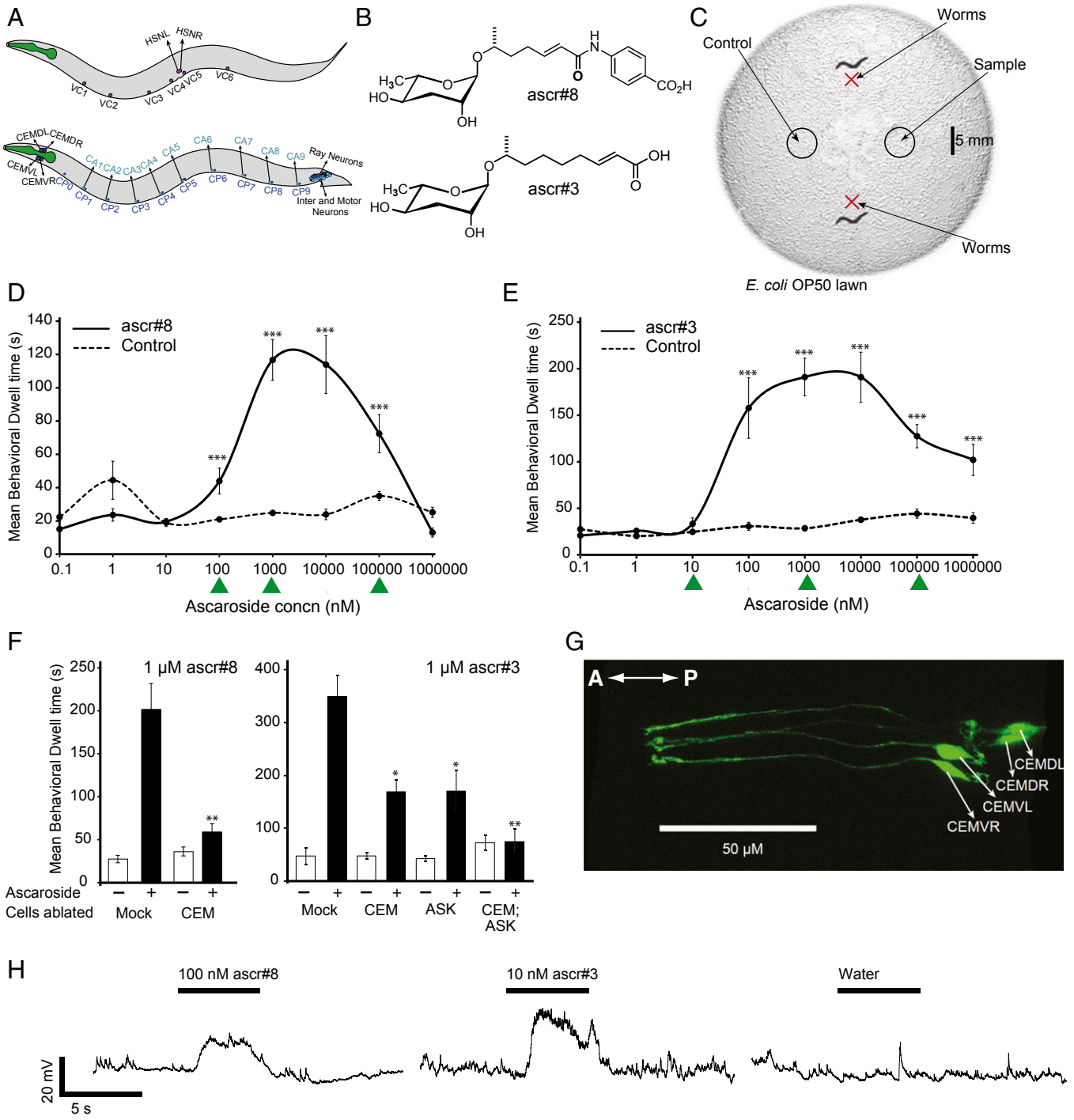

Fig. 1. Male-specific CEM neurons respond to multiple sex-specific ascarosides. (*A*) Sex-specific neurons in hermaphrodites (*Top*) and male *C. elegans* (*Bottom*). (*B*) Two ascarosides that are produced by the hermaphrodite, ascr#8 and ascr#3. (*C*) Behavioral assay used to determine attractiveness of ascarosides. (*D* and *E*) Behavioral tuning curve showing the mean behavioral dwell time at different concentrations of ascr#8 and ascr#3, respectively. Asterisks indicate responses significantly greater than controls with buffer, $P < 0.0001$, Student's *t* test. Concentrations without asterisks were not significantly different from controls. Green arrowheads indicate concentrations of ascaroside used for electrophysiological analyses. (*F*) Ablation of male-specific CEM neurons abolishes attraction to ascr#8 (*Left*) and reduces attraction to ascr#3 (*Right*). Data for ascr#3 has been reported by us (23). (*G*) CEM neurons labeled with green fluorescent protein (GFP) in adult male worm expressing *pkd-2::gfp*. (*H*) CEM neurons show responses to ascr#8 and ascr#3 but not to water. Black, example traces.

develop and maintain its concentration preferences. We find that *C. elegans* employs a novel mechanism of heterogeneous responses combined with concentration-dependent kinetics within a primary sensory neuron class to build a concentration tuning curve and likely uses synaptic modulation to do so.

Results

Male-Specific CEM Neurons Respond to Both ascr#3 and 8. Of the ascarosides tested, we found male *C. elegans* have the strongest responses to ascarosides #3 and #8 (ascr#3 and ascr#8, respectively; Fig. 1*B*), in a two-choice behavioral assay (Fig. 1*C*).

Worms had strong preferences for specific concentrations of the ascarosides, resulting in characteristic behavioral tuning curves (Fig. 1 *D* and *E*). Our cell ablation experiments indicated that male response to ascr#3 requires two classes of neurons, amphid sensory neuron class K (ASK) and CEM (Fig. 1*F, Right*) (23). ASK is common to both sexes, whereas CEM is a set of four male-specific cephalic sensory neurons (CEM dorsal/ventral, left/right; Fig. 1*G*). Additional ablation experiments indicate that the response to ascr#8 is mediated primarily by CEMs (Fig. 1*F, Left*). We established a whole-cell patch clamp preparation (25, 26) for the CEMs and performed electrophysiological recordings. We confirmed that the CEMs responded to both ascr#3 and ascr#8 but not to water (Fig. 1*H*).

CEM Neurons Show Three Modes of Responses to Ascarosides. To measure the evoked electrical currents in CEMs in response to different concentrations of ascr#8, we performed voltage clamp recordings. CEM responses fell on a continuum that crosses zero: while individually recorded neurons had stereotyped responses, the responses across the population varied in magnitude and sign (Fig. 2*A* and *SI Appendix*, Fig. S1 *A* and *B*). We classified the responses as depolarizing, hyperpolarizing, or no response (population averaged trials shown in Fig. 2*C*; example traces in Fig. 2*B* and *SI Appendix*, Fig. S2). The depolarizing and hyperpolarizing responses do not covary across concentration: The depolarizing current peaks at intermediate concentration of ascr#8, which is the behaviorally most attractive, whereas the hyperpolarizing current is strongest at the highest tested concentration, which is behaviorally less attractive (Figs. 1*D* and 2*D*). The mode of response was depolarizing for approximately half the cells, regardless of the neuron's anatomical identity (Fig. 2*E*; see also *SI Appendix*, Fig. S3). Similarly, CEM responses to ascr#3 fall on a continuum crossing zero, and also can be classified into three modes (Fig. 3 *A* and *C* and *SI Appendix*, Fig. S1 *C* and *D*; example traces in Fig. 3*B* and *SI Appendix*, Fig. S4) uncorrelated with the anatomical identity of the recorded CEM (Fig. 3*D* and *SI Appendix*, Fig. S5). The depolarizing current also peaks at intermediate concentrations corresponding to the behavioral tuning curve (Figs. 1*E* and 3*D*).

A few neurons had complex responses with both depolarizing and hyperpolarizing responses, sometimes within the same trial and sometimes on successive trials (ascr#8, 4/114 neurons, 3.5% of dataset; ascr#3, 11/90 neurons, 12% of dataset, example neurons *SI Appendix*, Figs. S6 and S7). To observe membrane voltage fluctuations evoked by ascaroside application, we performed current clamp recordings of CEMs. We observed large depolarizations and hyperpolarizations (20–40 mV changes) as well as fast transient events (Fig. 1 and *SI Appendix*, Fig. S8).

Intact Worms Have Access to Both Depolarizing and Hyperpolarizing CEM Signals. To test whether a given worm could potentially have access to both depolarizing and hyperpolarizing CEM signals, we recorded responses to ascr#8 from two different CEMs in the same worm (*SI Appendix*, Fig. S9), and found that in fact, different neurons in the same worm have different modes of response in two-thirds of all cases. To confirm that an intact worm can have simultaneous access to differently signed CEM signals, we imaged the ascaroside responses of all four CEMs from individual worms expressing the genetically encoded calcium indicator GCaMP (Fig. 4 and *SI Appendix*, Figs. S10–S13 and Movies S1 and S2). Individual CEMs from a single worm did not all have the same mode of response to ascaroside (Fig. 4 *A* and *B* and *SI Appendix*, Fig. S14). There were approximately twice as many cells exhibiting an ascaroside-evoked Ca^{2+} increase as there were exhibiting an ascaroside-evoked Ca^{2+} decrease.

CEM Responses Are Shaped by Synaptic Input. To test whether network synaptic input played a role in generating heterogeneous CEM responses, we recorded CEM responses to the high concentrations of ascarosides in worms deficient in UNC-13, a syntaxin-binding protein that is necessary for fast synaptic transmission. We used the *unc-13(s69)* mutant that lacks both isoforms of UNC-13 and has virtually no fast synaptic transmission (27). We found that the depolarizing responses to ascr#8 were enhanced in the absence of fast synaptic transmission, confirming our hypothesis that synaptic feedback plays a role in ascaroside representation (Fig. 5*A*). Further, we note that the depolarizing *unc-13* responses to ascr#8 were orders of magnitude larger than wild-type ascr#8 responses, responses to ascr#3, and nondepolarizing *unc-13* responses (Fig. 5*A* and *SI Appendix*, Figs. S2, S4, and S15). This range suggests that there could be large-scale synaptic feedback in the processing of ascr#8 responses.

The hyperpolarizing responses to ascr#8 were also enhanced by the removal of synaptic transmission, although not to the same extent as the depolarizing responses (Fig. 5*A* and *SI Appendix*, Figs. S2 and S15*A*). This enhancement suggests that the hyperpolarizing mode of response is not entirely due to fast synaptic transmission. The hyperpolarizing response could be the result of specific properties of ascaroside receptors, arise from peptidergic synaptic transmission, or arise from electrical coupling.

Responses to ascr#3 were sculpted by synaptic input of opposing signs although the magnitude of responses was unchanged (Fig. 5*B* and *SI Appendix*, Fig. S15). It thus appears that while processing ascr#3, CEMs could receive both excitatory and inhibitory fast synaptic input that is in opposition to the "mode" of the neuronal response (*SI Appendix*, Fig. S15*E* shows the average synaptic currents). Further, there were only two types of ascr#3 responses recorded in *unc-13* animals—depolarizing and hyperpolarizing (Fig. 5*C*).

A Single CEM Alone Cannot Generate the Behavioral Tuning Curve. The mean behavioral dwell time (Fig. 1 *D* and *E*) conflates two factors: one, how much time worms as a group spend in the ascaroside sample versus the control sample (which can be dominated by individual dwell-time values) and two, the number of worms significantly attracted to the chemical. We attempted to separate these two variables to better understand the behavior. First, to calculate the overall group attraction of worms to ascaroside versus control, we computed an Attraction Index, by computing the fraction of time spent in the ascaroside sample of the entire time spent in sample and control spots for all of the worms from a given behavioral session. As expected, this measure was consistently high across all concentrations for ascr#8 (*SI Appendix*, Fig. S16*A, Left*). Next, to estimate the fraction of total worms tested that exhibit attraction to ascaroside, we computed the percentage value of worm forays or runs into the ascaroside sample that were attractive [i.e., time spent in sample > (average time spent in control + 2 SDs)]. At intermediate concentrations, almost 90% of worm forays into ascaroside zones were significantly longer than forays into control zones, as opposed to only 30% of forays at other concentrations of ascr#8 (Fig. 6*A*, *Left*). These results suggest that animals are better able to restrict their movement to the ascaroside zone for intermediate concentrations compared with the others.

We tested the effect of eliminating all but one of the CEMs on behavior at different concentrations of ascarosides ("low," "medium," and "high"; green arrows in Fig. 1 *D* and *E*). We found that animals having only one surviving CEM had improved ascaroside attraction, but a flattened tuning curve—they were more attracted at low and high concentrations of ascaroside, rather than less attracted at all concentrations of ascr#8 (Fig. 6*A* and *SI Appendix*, Figs. S16*A* and S17). Having all four CEMs intact, in effect, appears to allow the worm to effectively locate an intermediate, possibly preferred concentration, resulting in

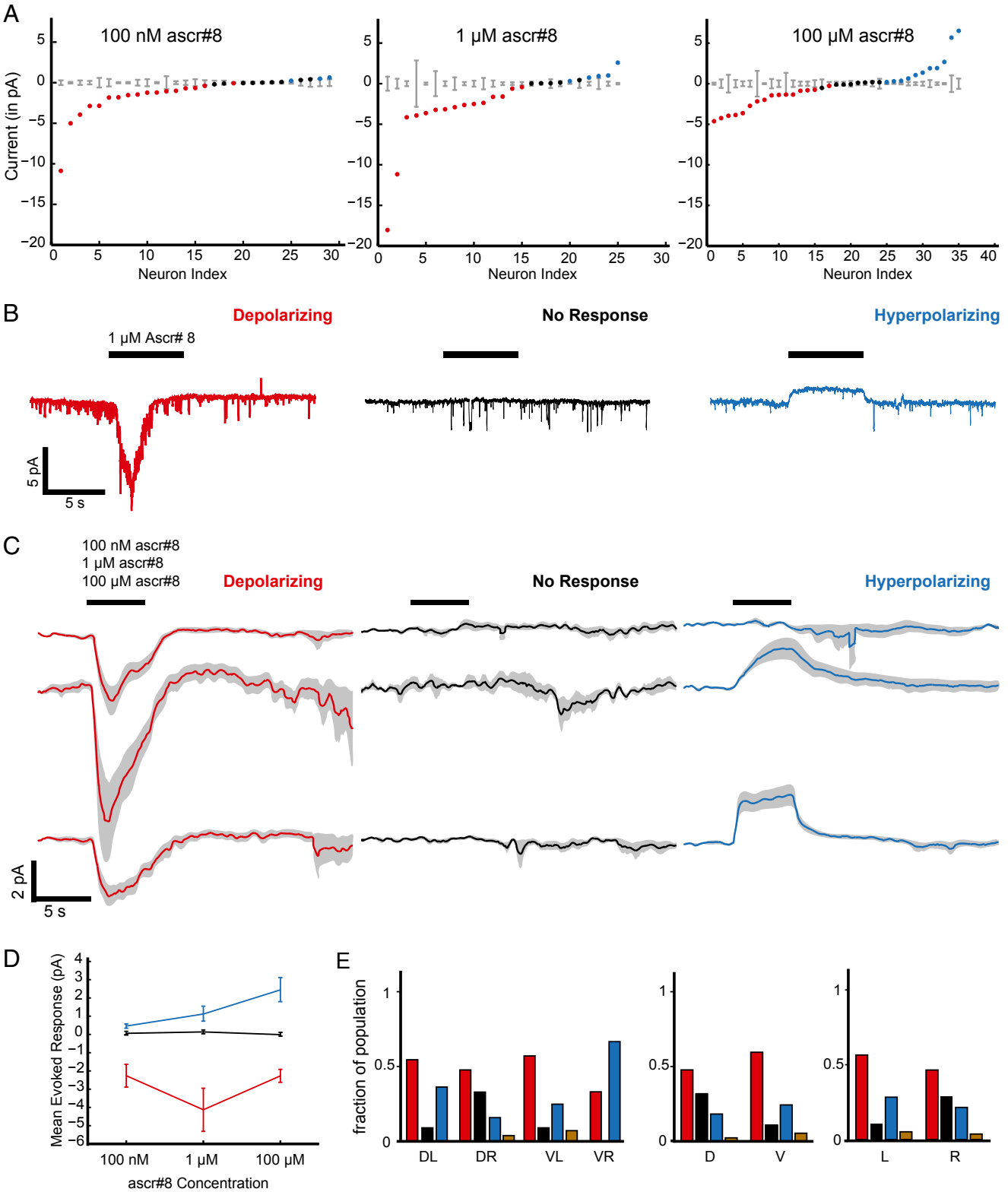

Fig. 2. CEM shows three modes of responses to ascr#8. (*A*) Mean-evoked current responses of neurons to 100 nM, 1 μM, and 100 μM concentrations of ascr#8 (columns). Each animal was only tested for a single concentration of ascaroside. A given neuron's response was classified as depolarizing (red), hyperpolarizing (blue), or not responsive (black), based on whether the average neural response over the duration of the stimulus exceeded 2× SD of the baseline (computed over 4 s before stimulus, shown in gray) for that neuron. (*B*) Example traces of different modes of response for 1 μM ascr#8, (*C*) Average evoked response over all cells for each mode of response (columns, colors as described for *A*) at 100 nM, 1 μM, and 100 μM concentrations of ascr#8 (rows). Solid line, population mean traces, gray, SEM. (*D*) Mean evoked current in each mode at different concentrations of ascr#8. (*E*) Neural response modes, pooled across concentrations. (*Left*) Grouped by individual CEM subclass. (*Middle*) Grouped into dorsal and ventral neurons. (*Right*) Grouped into left and right neurons. Brown bar represents complex responses (4 of 114 neurons in total).

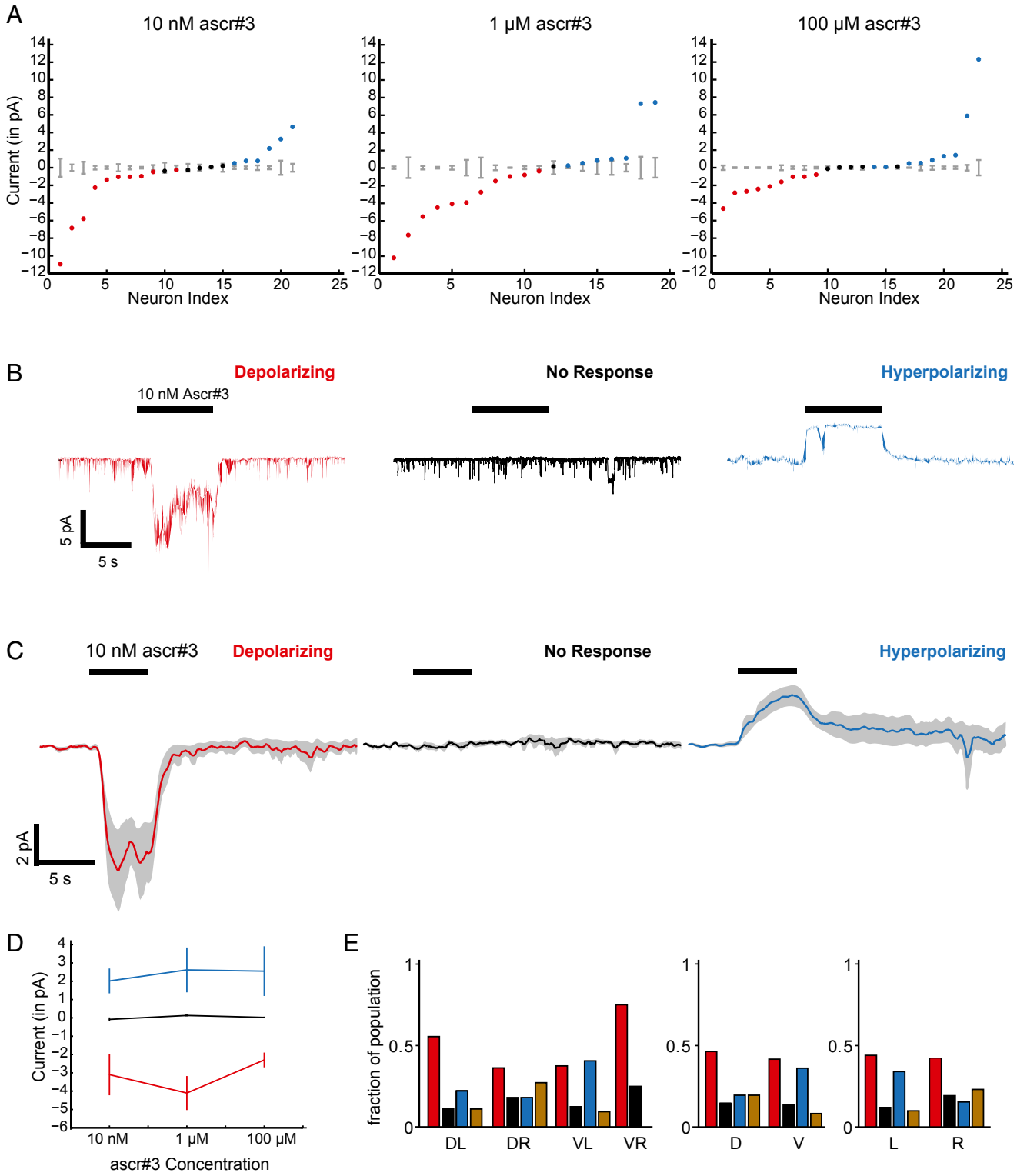

Fig. 3. CEM also shows three modes of responses to ascr#3. (*A*) Mean evoked current responses of neurons to 10 nM, 1 μM, and 100 μM concentrations of ascr#3 (columns). Each animal was only tested for a single concentration of ascaroside. A given neuron's response was classified as depolarizing (red), hyperpolarizing (blue), or not responsive (black), based on whether the average neural response over the duration of the stimulus exceeded 2× SD of the baseline (computed over 4 s before stimulus, shown in gray) for that neuron. (*B*) Example traces of different modes of response for 10 nM ascr#3, (*C*) Average evoked response over all cells for each mode of response (columns) at 10 nM ascr#3. Solid line, population mean traces, gray, SEM. (*D*) Mean evoked current in each mode at different concentrations of ascr#3. (*E*) Neural response modes, pooled across concentrations. (*Left*) Grouped by individual CEM subclass. (*Middle*) Grouped into dorsal and ventral neurons. (*Right*) Grouped into left and right neurons. Brown bar represents complex responses (11 of 90 neurons in total).

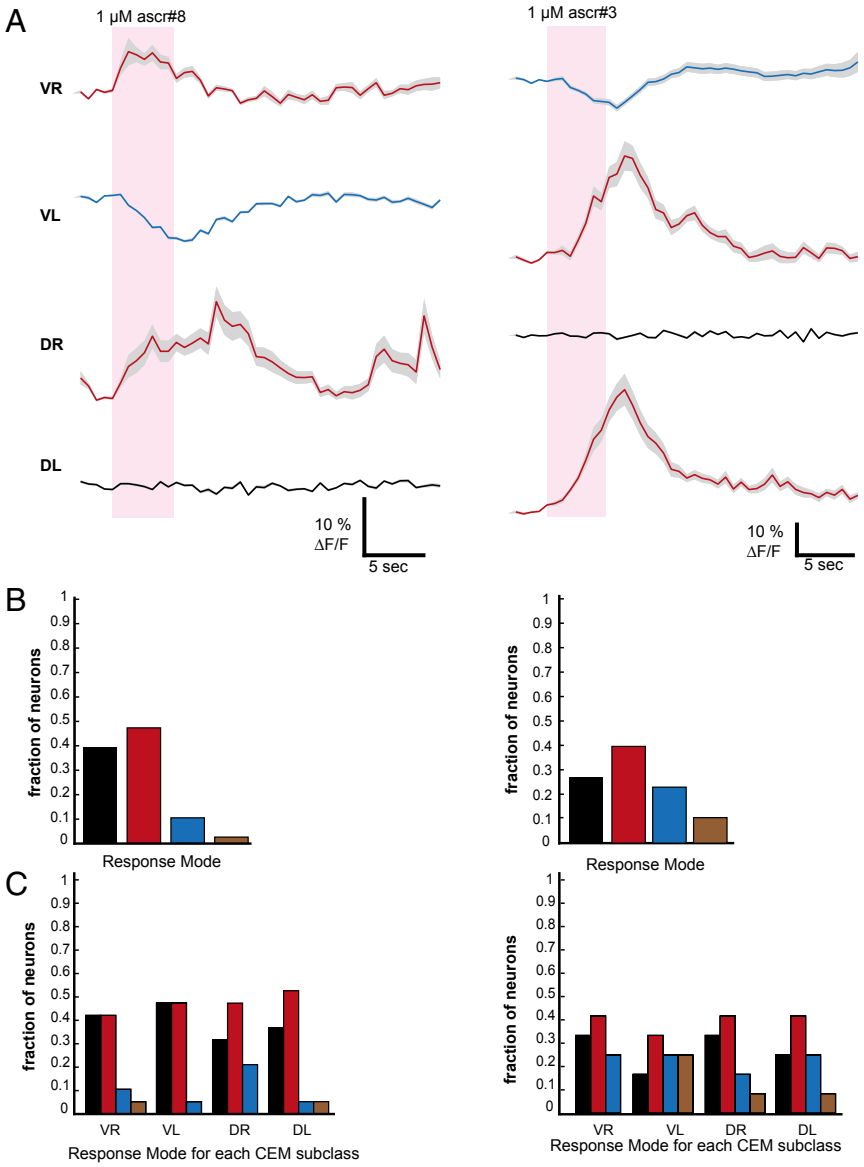

Fig. 4. GCaMP imaging corroborates heterogeneity of CEM responses to ascarosides within individual worms and within CEM subclasses. (*A*) Example calcium transients recorded simultaneously from all four CEMs in one animal exposed to 1 μM ascr#8 (*Left*) and responses of another animal to 1 μM ascr#3 (*Right*). A given neuron's response was classified as depolarizing (red), hyperpolarizing (blue), or not response (black) based on whether the average Δ*F*/*F* over the duration of the stimulus exceeded the average baseline Δ*F*/*F* + 2× SD preceding stimulus. Solid line, average over 10 trials; gray, SEM. Some cells are depolarized, whereas others are hyperpolarized. Neural response modes, pooled across animals (*B*) and grouped by individual CEM subclass (*C*), for ascr#8 (*Left*; $n = 72$ CEMs from 18 worms) and ascr#3 (*Right*; $n = 48$ CEMs from 12 worms). Brown bar represents fraction of cells that showed both depolarizing and hyperpolarizing responses in different subcellular compartments (see *Methods* for analysis details).

the observed concentration-tuning curve. Animals with no intact CEMs showed little to no response to ascr#8 (Fig. 6*A*, *Right*).

We computed similar behavioral metrics for ascr#3 (Fig. 6*B* and *SI Appendix*, Figs. S16*B* and S18). For ascr#3, the tuning curves are not as disrupted in worms with only one intact CEM (Fig. 6*B*, *Middle* and *SI Appendix*, Figs. S16*B* and S18). Further, animals with no intact CEMs show a diminished but intact tuning curve to ascr#3 (Fig. 6*B*, *Right*). This retained tuning possibly because the male response to ascr#3 is mediated both by CEMs and another sensory neuron class, ASK (Fig. 1*F*).

Previous work (28) using a different assay indicated that in concentrations ranges less than 50 pM, worms can chemotax in an ascr#3 gradient but not an ascr#8 gradient. This finding corroborates our results for ascr#8, because we show that the preferred concentration range for ascr#8 is 1 μM. The fact that worms can sense an ascr#3 gradient at low concentration further strengthens our hypothesis that the response to ascr#3 is more complex, involving other pathways, for instance ones originating from the neuron ASK.

Given that worms with one intact CEM are no longer able to distinguish concentrations, it is possible that the combined heterogeneous representation of the pheromone across all CEMS contributes to the encoding of concentration. We analyzed the kinetics of the CEM responses, by calculating the rise times (time for current to go from 10 to 90% of peak value) and the half-widths (interval elapsed between 50% of peak response on rising and falling phases of response). The hyperpolarizing response significantly lagged the depolarizing response at intermediate concentrations of ascr#8, but not at other concentrations (*SI Appendix*, Fig. S19*A*). For ascr#3, there is no significant lag

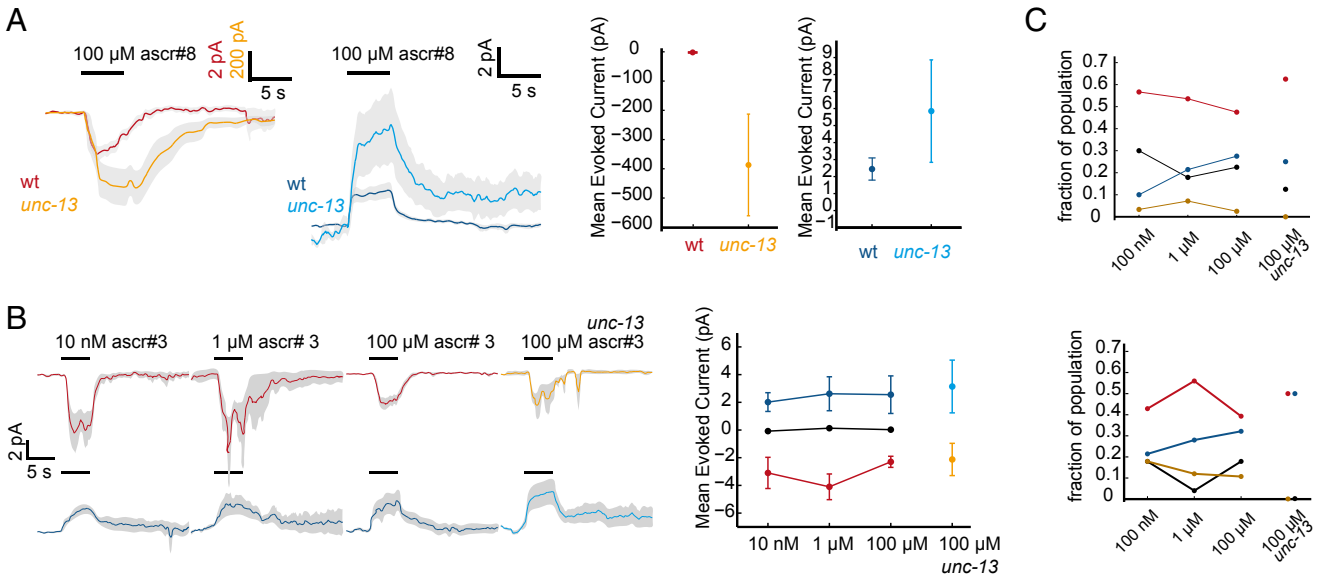

Fig. 5. CEM responses are shaped by synaptic input. (*A*) Lack of synaptic input enhances the ascaroside responses of both depolarizing and hyperpolarizing CEMs. Blue, wild-type hyperpolarizing response; cyan, *unc-13* hyperpolarizing response; orange, *unc-13* depolarizing response; red, wild-type depolarizing response. (*B*) Absence of synaptic input changes the shape but not magnitude of the neuronal response to ascr#3. Mean depolarizing response to ascr#3 shows a double-peaked structure (*Top*, first and second columns) that vanishes at high concentrations (third column) but reappears in *unc-13* animals. In neurons showing a hyperpolarizing response, the double-peaked structure vanishes in *unc-13* mutants. (*C*) Population fraction of each response mode at different concentrations. black, no response mode; blue, hyperpolarizing mode; brown, complex response mode; red, depolarizing mode.

between depolarizing and hyperpolarizing rise times at intermediate concentrations (*SI Appendix*, Fig. S20).

Discussion

Receptor neurons in a variety of vertebrates and invertebrates have shown both odor-evoked excitation and inhibition (1, 29, 30), but this finding has not hitherto been reported in *C. elegans*. We show that a given ascaroside can evoke both excitation and inhibition in a single neuron class with some neurons exhibiting both or neither. The underlying response continuum (Figs. 2*A* and 3*A*) could be generated by ascaroside-evoked currents summing with oppositely signed synaptic feedback. Variation in the delay with which the feedback is received at a given CEM could generate complex or nonresponsive cells. *unc-13* mutants, in fact, have virtually no nonresponsive or complex cells (Fig. 5*C* and *SI Appendix*, Fig. S15*F*), supporting the idea of such feedback summation. However, *unc-13*-mediated input does not account for the existence of hyperpolarizing responses in the first place. We show that peptidergic transmission may play a role, but we cannot rule out the existence of different ascaroside receptors, or second-messenger cascades (as in the lobster; ref. 31). Comparing response mode probabilities between wild-type and *unc-13* animals allows us to estimate the number of CEMs that are fundamentally depolarizing or hyperpolarizing for each ascaroside, and then indicate the manner in which *unc-13* input could change the response mode of these cells (Fig. 7*A*).

CEM response modes appear to be uncorrelated with anatomical identity. This lack of correlation suggests two possibilities. One, that CEMs are not members of a single class, However, as we discussed earlier in the Introduction, there is substantial anatomical and developmental evidence for CEMs to be considered a single class. The other possibility is that of stochastic expression of receptors (or other genetically encoded physiological properties) across the four CEMs in a single worm, as seen elsewhere in the *C. elegans* sensory network (13).

We show that synaptic feedback strongly inhibits the CEM response, and that the absence of three of four CEMs strongly increases ascaroside attraction at previously nonpreferred concentrations. This finding suggests that the CEMs might inhibit each other. In the current version of the male *C. elegans* connectome, the CEMs are not recurrently interconnected (wormwiring.hpc.einstein.yu.edu/male/male.php). However, almost all other classes of neurons in *C. elegans* have intraclass gap junctions and there is extensive recurrent multisynaptic connectivity (8, 32, 33), so a recurrent inhibition mechanism is not inconceivable.

The concentration tuning curves for *C. elegans* males thus appears to be actively set as a result of the combined responses of the CEM network. Concentration preferences can reflect important environmental cues and constraints. Very low and very high concentrations could imply limited resources or overcrowding. Further, both males and females could produce different levels of the same pheromone, as seen in mice (7), making some threshold selection mechanism necessary. In fact, we now have evidence that male *C. elegans* also produce some ascr#3 at a lower concentration (21).

Our analyses of response kinetics show that depolarizing responses are faster than hyperpolarizing responses at intermediate concentrations of ascr#8. Such a combination of fast excitation followed by slow inhibition could provide a derivative of the input signal (Fig. 7*B*), provided that a given worm has access to both the depolarizing and hyperpolarizing CEM signals (which we have shown is possible). We found that the composite CEM response (summing excitatory and inhibitory responses) resembled a derivative (Fig. 7*C*) at intermediate but not high or low concentrations. If the kinetics of heterogeneous CEM responses at intermediate concentrations allow the computation of a derivative when the odor turns on or off in time, it could potentially also allow it to detect equivalent on and off boundaries in space. A worm would then be able to better determine when it enters and leaves the ascaroside zone and, thus, stay within the intermediate concentration zone (or on the scent track of a hermaphrodite). Computing a sensory derivative has been shown to allow *Drosophila* larvae to navigate odor gradients (34). A differentiator motif comprising a fast sensor in an excitatory pathway and a slow one in an inhibitory pathway has been described (35) and has been shown to be a viable strategy in

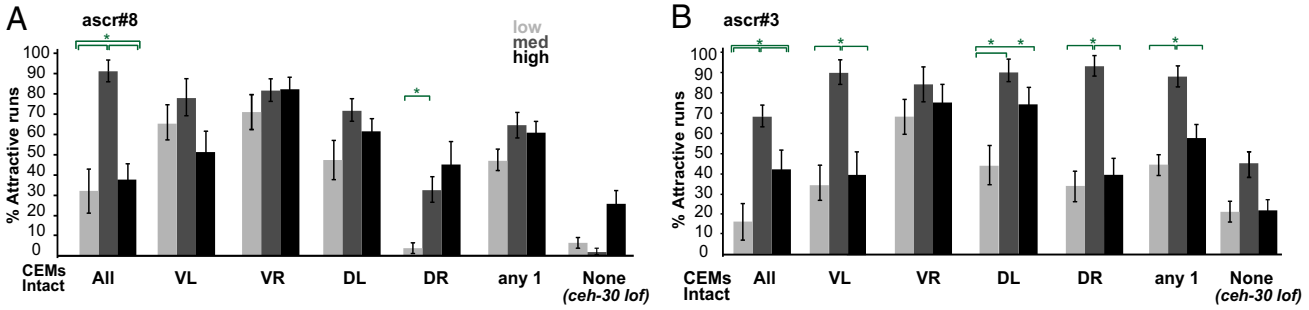

Fig. 6. A single CEM alone cannot generate the behavioral tuning curve. (*A*) Percentage of all forays that were attractive for ascr#8. From left to right, the conditions were as follows: intact worms, worms with only one of four CEMs intact (groups 2–5) and the average of all ablated worms, and worms with no intact CEMs. (*B*) Similarly organized data for ascr#3. All values mean ± SEM. All statistical comparisons performed by using one-way ANOVA with $P < 0.05$ followed by Tukey's HSD test for multiple comparisons. See *Methods* for statistical values.

computational models of *C. elegans* chemotaxis (36). The composite response of CEMs could be faithfully transmitted to the next stage of processing were the synaptic transfer function between CEMs and downstream neuron(s) to be graded and tonic, something that we and others have shown to be the case at other *C. elegans* synapses (26, 37). Further, given the variability in individual response kinetics and synaptic gain, it is probable that the differentiator "response" in each worm is slightly different, possibly leading to a variation in behavioral preferences. Such a natural variation could be beneficial for the population as a whole, allowing a more efficient exploration of parameter space.

This pattern is not evident for ascr#3; in particular, the tuning curves are not as disrupted in worms with only one intact CEM (Fig. 6*B*), there is no significant lag between depolarizing and hyperpolarizing rise times at intermediate concentrations, nor are the summed CEM responses highly similar to derivatives of step functions (*SI Appendix*, Fig. S20). As discussed previously, this lack of disruption in response to ascr#3 could be due to the fact that the ascr#3 sensing pathway is redundant, including both CEM and ASK.

For certain odors, it has been shown that the encoding of concentration in *C. elegans* is consistent with a labeled-line hypothesis, where different neurons respond to different concentrations (38). Our data suggest a previously uncharacterized strategy for pheromones, where the same set of four CEMs encode different concentrations in excitatory and inhibitory responses with varying kinetics. In bacterial models of chemotaxis, it has been shown that a biphasic response probability (with a short fast increase and a slower depression) allows the bacterium to reconcile the short-term goal of navigating up chemical gradients with the long-term goal of aggregating at peaks (39). We propose that the differences in the kinetics of the dissimilar CEM responses set up a signal differentiator only at intermediate concentrations, which could allow the animal to be attracted by all concentrations, yet actively prefer an intermediate one. Encoding different concentrations in dissimilar responses within a single neuronal class appears to be yet another method (13, 40, 41) by which nematodes, with their compact nervous systems, break symmetry to increase coding capacity.

Methods

Strains. CB1490 *him-5(e1490)* males were used in our bioassays and in neuron ablation experiments. This *him-5* mutant segregates XO male progeny by X chromosome nondisjunction during meiosis (42). The CB1490 males were not different from wild-type males in our bioassays. We used strain CU607 *smIs23 [pkd-2::gfp+ pBX]; him-5(e1490)* (43) to record responses from GFP-labeled CEM neurons. We crossed this *smIs23* transgene into BC168 [*unc-13(s69)*] to obtain strain PS6327, used to record responses in the *unc-13* synaptic mutant background. To perform calcium imaging experiments, we used a ppkd-2::GCAMP6 strain; *fkEx98[Ppkd-2::GCaMP::SL2::dsRED + pBX-1]; pha-1(e2123ts); him-5(e1490); lite-1(ce314)*.

Spot Retention Assays. Assays were done as described (23). For both *C. elegans* hermaphrodites and males, we harvested 50–60 worms daily at the fourth larval stage (L4) and stored them segregated by sex at 20 °C overnight to be used as young adults the following day. Because both ascr#3 and ascr#8 are water soluble, we made working solutions of these chemicals in double distilled water and stored aliquots at −20 °C in 20-μL tubes. As control, we used double distilled water.

Laser Ablations and Behavioral Assays. We used the late L2 larva stage for ablations of CEM neurons. We chose this larval stage because we were able to identify the cell body of CEM neurons robustly. Males were identified by checking for the presence of the B cell in the tail region (20), and CEM ablations were performed as described (23). A successful ablation was confirmed a few hours after recovery and did not exhibit any damage to neighboring neurons. We ablated CEM neurons at the L4 stage because it has been reported that CEM neurons undergo developmental changes during development (44). We did not observe any difference in response to ascr#3 and ascr#8 by CEM ablations at the L2 or the L4 stage.

We tested 10 ablated individuals in our spot retention assay four times. After each assay, we transferred the ablated animals from the assay plates onto plates containing copper rings for 1 h to reacclimatize. The same procedure was used for the mock-treated animals. The mean time spent in scoring region was computed for both sets of animals. Each ablation set was repeated at least on two separate days.

Electrophysiology. Worms were maintained in well-fed conditions at 20 °C. Experiments were performed at room temperature (~20 °C). Approximately 300 adult male *C. elegans* were picked to a fresh agar plate seeded with OP_{50} *E. coli* the day before each recording session. Worms were prepared for electrophysiology as described (25, 26). A glass pipette filled with ascaroside (or water for controls) and 9 μM sulforhodamine (for visualization) was positioned near the buccal cavity of the worm, and was connected to a Picopump (WPI) to deliver timed stimulus pulses adjacent to the head of the animal.

Whole-cell patch clamp recordings from 209 neurons (summed across all experiments) are included in this study. Each neuron was only tested for one pheromone condition. Only one neuron was recorded from each worm, except in the case of a subset ($n = 9$ worms) where we recorded from 2 CEMs. Only the first recorded CEM was included in the quantitative analyses to maintain comparability.

Before analysis, we discarded recordings according to the following quality criteria: (*i*) cell damage or stimulus delivery malfunction (assessed by visual inspection), (*ii*) poor seal resistance values (threshold >1 Gohm), and (*iii*) unstable baseline, as measured by the SD of the baseline noise. Recordings where the baseline (4 s before stimulus onset) SD was greater than twice that of the mean population were eliminated.

Solutions: Internal buffer: 143 mM KAsp, 0.1 mM $CaCl_2$, 1.1 mM EGTA, 10 mM Hepes, 15 μM sulforhodamine, 4 mM MgATP, 0.5 mM Na_3GTP, pH 7.2, osmolarity ~310 mOsm. External buffer: 145 mM NaCl, 5 mM KCl, 5 mM $MgCl_2$, 1 mM $CaCl_2$, 10 mM Hepes, pH 7.2, osmolarity ~320 mOsm.

Patch electrodes were pressure-polished for a tip resistance of 5–15 MΩ. Recordings were not corrected for junction potential (calculated to be 17 mV for the control solutions used) and series resistance. Clamp voltage for voltage clamp experiments was −65 mV.

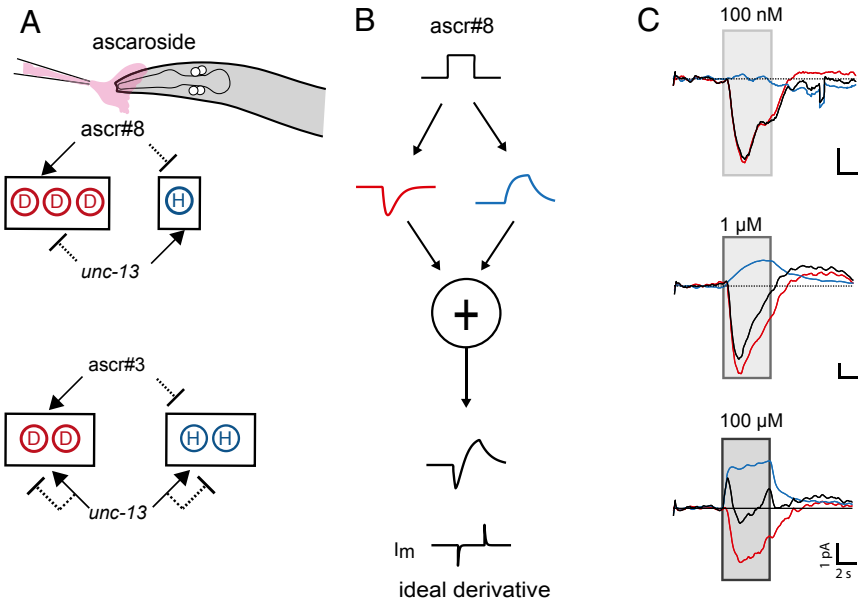

Fig. 7. A combination of fast excitation and slow inhibition could allow CEM to serve as a signal differentiator at optimal concentrations. (*A*) Model showing the grouping of cells and the effect of ascarosides #8 and #3 along with synaptic input. D and H indicate individual CEMs that are hypothesized to be natively depolarized or hyperpolarized in the absence of fast synaptic input. (*B*) The combination of fast excitation and slow inhibition suggests a role for the CEM class as a signal differentiator. (*C*) The effective CEM output looks most like a derivative of the input at intermediate concentrations, to which the worm is most attracted. Black traces, sum of the excitatory and inhibitory responses; blue, averaged inhibitory response; red traces, averaged excitatory response.

Data were acquired at 15 kHz by using the Patchmaster program and a HEKA EPC-10 patch clamp amplifier, and filtered at 3 kHz. Analysis was performed by using custom software written in MATLAB.

Calcium Imaging. We used an inverted spinning disk confocal microscope with a 488-nm laser to image changes in fluorescence in worms expressing GCaMP6s under the control of *pkd-2* 5′ regulatory sequences in CEM neurons fkEx98[Ppkd-2::GCaMP::SL2::dsRED + pBX-1]; *pha-1(e2123ts); him-5(e1490); lite-1(ce314)*. Worms were washed in Nematode Growth Medium (NGM) buffer and restrained in a modified version of the microfluidic chip described in ref. 45, with a smaller channel to accommodate male worms. Further immobilization to enable the image segmentation of individual CEM neurons and minimize motion artifacts was achieved by adding 100 nM tetramisole to the NGM buffer. Odors were delivered by using a valve manifold with switching times on the order of 5–10 ms. Worms were stimulated by using different ascaroside solutions, containing an additional 150 nM fluorescein sodium to visualize the stimulus pulse.

We recorded calcium responses from 34 worms. In each worm, we imaged a volume 30 μm deep encompassing all four CEMs and their processes. To analyze the fluorescence intensity changes, each movie was annotated for features of interest. Up to four features were annotated for each CEM (dendrite tip, dendrite, soma, and ring neurite), for a total of up to 16 possible features from each worm. Feature volumes of interest were tracked across successive time steps to correct for motion by using custom software written in MATLAB. The fluorescence intensity was computed as the average pixel intensity of the 10 brightest pixels from each frame for each feature. Trials were then stimulus aligned, and each feature was classified as showing excitation, inhibition, or no response based on whether the average Ca $\Delta F/F$ over the duration of stimulation exceeded 2 SD of the mean-subtracted baseline. Worms where no features showed any sign of activation across all cells were excluded from further analysis (4 of 34 worms). Each cell was then assigned a response mode as follows. A cell that had nonresponsive features and depolarizing (hyperpolarizing) features was classified as depolarizing (hyperpolarizing). A cell that had both depolarizing and hyperpolarizing features was classified as complex. Example intensity traces described in Fig. 6 are from individual features.

Statistical Analyses. Statistical comparisons were made by one-way analysis of variance with significance level set at 0.05, followed by post hoc Tukey's Honest Significant Difference (HSD) tests. We used unpaired Student's *t* tests with Welch's correction for comparing attraction of males on the different ascarosides, $*P < 0.01$, $**P < 0.001$, $***P < 0.0001$.

Statistical Values for Behavioral Comparisons from *SI Appendix*, Fig. S9.
Attraction Index, ascr#8 (SI Appendix, Fig. S14A). There was no significant difference between attractive indices across concentrations for intact animals at the $P < 0.05$ level [$F(2,37) = 1.73$, $P = 0.19$], animals with only dorsal left (DL) intact [$F(2,40) = 0.49$, $P = 0.61$], only dorsal right (DR) intact [$F(2,39) = 2.13$, $P = 0.13$], only ventral left (VL) intact [$F(2,40) = 2.54$, $P = 0.09$], only ventral right (VR) intact [$F(2,40) = 0.19$, $P = 0.83$], or pooled across ablations [$F(2,125) = 1.43$, $P = 0.24$].
%Attractive Runs, ascr#8 (Fig. 6A). There was a significant difference for intact animals across concentrations of ascr#8 at $P < 0.05$ [$F(2, 36) = 44.79$ value, $P = 1.7e{-}10$]. Post hoc Tukey's HSD test showed that the %attractive run values at all concentrations were significantly different from each other. There was no significant difference for animals with only 1 DL intact [$F(2,40) = 1.38$, $P = 0.2641$], 1 VL intact [$F(2,40) = 2.19$, $P = 0.1254$] or 1 VR intact [$F(2,40) = 0.69$, $P = 0.5075$). There was a significant difference for animals with only one DR intact [$F(2,39) = 7.12$, $P = 0.0023$]. Post hoc Tukey's HSD test showed a significant difference between concentrations 1 and 2 and concentrations 1 and 3, but not concentrations 2 and 3. Pooling all of the ablations showed a significant difference at $P < 0.05$ [$F(2,125) = 3.49$, $P = 0.03$]. Post hoc Tukey's HSD test showed that there was a significant difference between concentrations 1 and 2, but none of the other pairs.
Attraction Index, ascr#3 (SI Appendix, Fig. S14B). There was a significant difference in AI for intact ascr#3 at $P < 0.05$ [$F(2, 88) = 9.76$, $P = 0.0001$]. Post hoc Tukey's HSD test showed that the AI values at medium concentrations were significantly different from both low and high. There was a significant difference for animals with only 1 DL intact [$F(2,42) = 9.61$, $P = 0.0004$]. Post hoc Tukey's HSD test showed that the AI values at low concentrations were significantly different from the medium concentrations. There was a significant difference for animals with only 1 DR intact [$F(2,42) = 14.55$, $P = 1.57e{-}05$]. Post hoc Tukey's HSD test showed that the AI values at medium concentrations were significantly different from the low as well as high concentrations. There was a significant difference for animals with only 1 VL intact [$F(2,42) = 8.49$, $P = 0.0008$]. Post hoc Tukey's HSD test showed that the Attraction Index (AI) values at medium concentrations were significantly different from the low as well as high concentrations. There was no significant difference for animals with only 1 VR intact [$F(2,40) = 1.2$, $P = 0.3125$. Pooling all of the ablations showed a significant difference at $P < 0.05$ [$F(2,132) = 22.13$, $P = 5.14e{-}9$]. Post hoc Tukey's HSD test showed that AI values at medium concentrations were significantly different from the low as well as high concentrations.
% of Attractive Runs, ascr#3 (Fig. 6B). There was a significant difference in %Attractive runs for intact animals across concentrations of Ascr#3 at $P < 0.05$ [$F(2, 88) = 16.67$, $P = 7.26e{-}7$]. Post hoc Tukey's HSD test showed that the

%attractive run values at all concentrations were significantly different from each other. There was a significant difference for animals with only 1 DL intact [$F(2,42) = 8.05$, $P = 0.0011$]. Post hoc Tukey's HSD test showed that the %attractive run values at low concentrations were significantly different from the medium and high concentrations. There was a significant difference for animals with only 1 DR intact [$F(2,42) = 16.08$, $P = 5.81e{-}6$]. Post hoc Tukey's HSD test showed that the %attractive run values at medium concentrations were significantly different from the low and high concentrations. There was a significant difference for animals with only 1 VL intact [$F(2,42) = 10.53$, $P = 0.0002$]. Post hoc Tukey's HSD test showed that the %attractive run values at medium concentrations were significantly different from the low as well as high concentrations. There was no significant difference for animals with only 1 VR intact [$F(2,40) = 0.56$, $P = 0.5733$]. Pooling all of the ablations showed a significant difference at $P < 0.05$ [$F(2,132) = 30.01$, $P = 1.8e{-}11$]. Post hoc Tukey's HSD test showed that % attractive run values at medium concentrations were significantly different from the low as well as high concentrations.

ACKNOWLEDGMENTS. We thank Ofer Mazor, Michale Fee, and Vivek Jayaraman for helpful suggestions; Scott Emmons for sharing unpublished information on the male connectome; and Robyn Lints for the generous gift of the *ppkd-2*::GCAMP6 strain. This work was supported in part by National Science Foundation Grant PHY-0957185 and National Institutes of Health (NIH) Grant 8DP1GM105383-05 (to A.D.T.S.), startup funds from Worcester Polytechnic Institute (to J.S.), NIH Grant GM085285 (to F.C.S. and P.W.S.), and the Howard Hughes Medical Institute, with which P.W.S. is an Investigator.

1. Ache BW, Young JM (2005) Olfaction: Diverse species, conserved principles. *Neuron* 48(3):417–430.
2. Bargmann CI (2006) Comparative chemosensation from receptors to ecology. *Nature* 444(7117):295–301.
3. Wilson RI (2008) Neural and behavioral mechanisms of olfactory perception. *Curr Opin Neurobiol* 18(4):408–412.
4. Jayaraman V, Laurent G (2009) Olfactory system: Circuit dynamics and neural coding in the locust. *Encyclopedia of Neuroscience*, ed Squire LR (Academic, Oxford), pp 187–196.
5. Mori K, Nagao H, Yoshihara Y (1999) The olfactory bulb: Coding and processing of odor molecule information. *Science* 286(5440):711–715.
6. Soucy ER, Albeanu DF, Fantana AL, Murthy VN, Meister M (2009) Precision and diversity in an odor map on the olfactory bulb. *Nat Neurosci* 12(2):210–220.
7. Brennan PA, Keverne EB (2004) Something in the air? New insights into mammalian pheromones. *Curr Biol* 14(2):R81–R89.
8. White JG, Southgate E, Thomson JN, Brenner S (1986) The structure of the nervous system of the nematode Caenorhabditis elegans. *Philos Trans R Soc Lond B Biol Sci* 314(1165):1–340.
9. Jarrell TA, et al. (2012) The connectome of a decision-making neural network. *Science* 337(6093):437–444.
10. Sammut M, et al. (2015) Glia-derived neurons are required for sex-specific learning in C. elegans. *Nature* 526(7573):385–390.
11. Sulston JE, Horvitz HR (1981) Abnormal cell lineages in mutants of the nematode Caenorhabditis elegans. *Dev Biol* 82(1):41–55.
12. Suzuki H, et al. (2008) Functional asymmetry in Caenorhabditis elegans taste neurons and its computational role in chemotaxis. *Nature* 454(7200):114–117.
13. Wes PD, Bargmann CI (2001) C. elegans odour discrimination requires asymmetric diversity in olfactory neurons. *Nature* 410(6829):698–701.
14. Sulston JE, Schierenberg E, White JG, Thomson JN (1983) The embryonic cell lineage of the nematode Caenorhabditis elegans. *Dev Biol* 100(1):64–119.
15. Barr MM, et al. (2001) The Caenorhabditis elegans autosomal dominant polycystic kidney disease gene homologs lov-1 and pkd-2 act in the same pathway. *Curr Biol* 11(17):1341–1346.
16. Schwartz HT, Horvitz HR (2007) The C. elegans protein CEH-30 protects male-specific neurons from apoptosis independently of the Bcl-2 homolog CED-9. *Genes Dev* 21(23):3181–3194.
17. Hurd DD, Miller RM, Núñez L, Portman DS (2010) Specific alpha- and beta-tubulin isotypes optimize the functions of sensory Cilia in Caenorhabditis elegans. *Genetics* 185(3):883–896.
18. Barr MM, Sternberg PW (1999) A polycystic kidney-disease gene homologue required for male mating behaviour in C. elegans. *Nature* 401(6751):386–389.
19. Wang J, et al. (2015) Cell-specific transcriptional profiling of ciliated sensory neurons reveals regulators of behavior and extracellular vesicle biogenesis. *Curr Biol* 25(24): 3232–3238.
20. Sulston JE, Horvitz HR (1977) Post-embryonic cell lineages of the nematode, Caenorhabditis elegans. *Dev Biol* 56(1):110–156.
21. Izrayelit Y, et al. (2012) Targeted metabolomics reveals a male pheromone and sex-specific ascaroside biosynthesis in Caenorhabditis elegans. *ACS Chem Biol* 7(8):1321–1325.
22. von Reuss SH, et al. (2012) Comparative metabolomics reveals biogenesis of ascarosides, a modular library of small-molecule signals in C. elegans. *J Am Chem Soc* 134(3): 1817–1824.
23. Srinivasan J, et al. (2008) A blend of small molecules regulates both mating and development in Caenorhabditis elegans. *Nature* 454(7208):1115–1118.
24. Ludewig AH, Schroeder FC (2013) Ascaroside signaling in C. elegans. *WormBook* 1–22.
25. Goodman MB, Hall DH, Avery L, Lockery SR (1998) Active currents regulate sensitivity and dynamic range in C. elegans neurons. *Neuron* 20(4):763–772.
26. Narayan A, Laurent G, Sternberg PW (2011) Transfer characteristics of a thermosensory synapse in Caenorhabditis elegans. *Proc Natl Acad Sci USA* 108(23):9667–9672.
27. Richmond JE, Davis WS, Jorgensen EM (1999) UNC-13 is required for synaptic vesicle fusion in C. elegans. *Nat Neurosci* 2(11):959–964.
28. Choe A, et al. (2012) Ascaroside signaling is widely conserved among nematodes. *Curr Biol* 22(9):772–780.
29. Ache BW (2010) Odorant-specific modes of signaling in mammalian olfaction. *Chem Senses* 35(7):533–539.
30. Buck LB (1996) Information coding in the vertebrate olfactory system. *Annu Rev Neurosci* 19:517–544.
31. Boekhoff I, Michel WC, Breer H, Ache BW (1994) Single odors differentially stimulate dual second messenger pathways in lobster olfactory receptor cells. *J Neurosci* 14(5 Pt 2): 3304–3309.
32. Chen BL, Hall DH, Chklovskii DB (2006) Wiring optimization can relate neuronal structure and function. *Proc Natl Acad Sci USA* 103(12):4723–4728.
33. Reigl M, Alon U, Chklovskii DB (2004) Search for computational modules in the C. elegans brain. *BMC Biol* 2:25.
34. Schulze A, et al. (2015) Dynamical feature extraction at the sensory periphery guides chemotaxis. *eLife* 4:4.
35. Goentoro L, Shoval O, Kirschner MW, Alon U (2009) The incoherent feedforward loop can provide fold-change detection in gene regulation. *Mol Cell* 36(5):894–899.
36. Dunn NA, Conery JS, Lockery SR (2007) Circuit motifs for spatial orientation behaviors identified by neural network optimization. *J Neurophysiol* 98(2):888–897.
37. Lindsay TH, Thiele TR, Lockery SR (2011) Optogenetic analysis of synaptic transmission in the central nervous system of the nematode Caenorhabditis elegans. *Nat Commun* 2:306.
38. Yoshida K, et al. (2012) Odour concentration-dependent olfactory preference change in C. elegans. *Nat Commun* 3:739.
39. Clark DA, Grant LC (2005) The bacterial chemotactic response reflects a compromise between transient and steady-state behavior. *Proc Natl Acad Sci USA* 102(26): 9150–9155.
40. Pierce-Shimomura JT, Faumont S, Gaston MR, Pearson BJ, Lockery SR (2001) The homeobox gene lim-6 is required for distinct chemosensory representations in C. elegans. *Nature* 410(6829):694–698.
41. Yu S, Avery L, Baude E, Garbers DL (1997) Guanylyl cyclase expression in specific sensory neurons: A new family of chemosensory receptors. *Proc Natl Acad Sci USA* 94(7):3384–3387.
42. Hodgkin J, Horvitz HR, Brenner S (1979) Nondisjunction mutants of the nematode Caenorhabditis elegans. *Genetics* 91(1):67–94.
43. Peden E, Kimberly E, Gengyo-Ando K, Mitani S, Xue D (2007) Control of sex-specific apoptosis in C. elegans by the BarH homeodomain protein CEH-30 and the transcriptional repressor UNC-37/Groucho. *Genes Dev* 21(23):3195–3207.
44. White JQ, et al. (2007) The sensory circuitry for sexual attraction in C. elegans males. *Curr Biol* 17(21):1847–1857.
45. Chronis N, Zimmer M, Bargmann CI (2007) Microfluidics for in vivo imaging of neuronal and behavioral activity in Caenorhabditis elegans. *Nat Methods* 4(9):727–731.